Nonuniversal large-size asymptotics of the Lyapunov exponent in turbulent globally coupled maps

David Velasco, Juan M. López, and Diego Pazó*
Instituto de Física de Cantabria (IFCA), CSIC-Universidad de Cantabria, 39005 Santander, Spain
(Dated: September 15, 2021)

Globally coupled maps (GCMs) are prototypical examples of high-dimensional dynamical systems. Interestingly, GCMs formed by an ensemble of weakly coupled identical chaotic units generically exhibit a hyperchaotic 'turbulent' state. A decade ago, Takeuchi *et al.* [Phys. Rev. Lett. **107**, 124101 (2011)] theorized that in turbulent GCMs the largest Lyapunov exponent (LE), $\lambda(N)$, depends logarithmically on the system size N: $\lambda_\infty - \lambda(N) \simeq c/\ln N$. We revisit the problem and analyze, by means of analytical and numerical techniques, turbulent GCMs with positive multipliers to show that there is a remarkable lack of universality, in conflict with the previous prediction. In fact, we find a power-law scaling $\lambda_\infty - \lambda(N) \simeq c/N^\gamma$, where γ is a parameter-dependent exponent in the range $0 < \gamma \leq 1$. However, for strongly dissimilar multipliers, the LE varies with N in a slower fashion, which is here numerically explored. Although our analysis is only valid for GCMs with positive multipliers, it suggests that a universal convergence law for the LE cannot be taken for granted in general GCMs.

I. INTRODUCTION

Scaling laws pervade physics. In particular, in the field of chaos theory, universal routes to low-dimensional chaos with specific scaling properties were already discovered long time ago [1]. In contrast, high-dimensional chaos— observed in systems with many "active" degrees of freedom— remains only partly understood [2], and scaling laws are often based on more or less heuristic arguments. Regarding discrete time systems, certain scaling laws have been found for coupled-map lattices [3–5] and globally coupled maps (GCMs) [6, 7].

Concerning GCMs, a rich repertoire of phenomena are known [8, 9], including multistability, clustering, chimera or turbulence. Here, we focus on the turbulent regime in GCMs found at weak coupling. The study of turbulent GCMs extends over several decades. An early striking discovery was the nonstationarity of the mean field in the infinite size limit [9–12]. Subsequently, several papers characterized the collective properties of chaos in turbulent GCMs [13–16]. Finally, Takeuchi et al. [7] uncovered the delicate arrangement of the Lyapunov exponents underlying turbulent GCMs: The Lyapunov spectrum is apparently extensive, but "subextensive bands" persist for arbitrarily large system sizes at both ends of the Lyapunov spectrum. In the same work [7], see also Chap. 11 of [17], a partially analytic treatment concluded that the largest Lyapunov exponent (LE) λ converged to its asymptotic value λ_∞ logarithmically with the system size N:

$$\lambda_\infty - \lambda(N) \simeq \frac{c}{\ln N}. \tag{1}$$

Here c is a positive constant, and the symbol $\simeq$ denotes equality after neglecting marginal contributions in N.

In this paper, we study turbulent GCMs with positive multipliers, finding that the LE converges to its infinite-size limit in a strongly nonuniversal manner. We show that, depending on the coupling strength and multipliers statistics, the LE can follow either a power law

$$\lambda_\infty - \lambda(N) \simeq \frac{c}{N^\gamma} \qquad \text{with } 0 < \gamma \leq 1, \tag{2}$$

or still a different, arguably slower, convergence law with N in certain situations.

Our results have important implications for turbulent GCMs with multipliers adopting both signs. The theoretical approach developed in [7], and claimed to support the scaling law (1), did not require any condition on the sign of the multipliers. Still, for positive multipliers, we find a different scaling law, given by Eq. (2). We solve this conflict by re-thinking the theoretical analysis done by Takeuchi et al. [7] and pointing out a loophole in their argumentation. In consequence, the actual asymptotic scaling law of the LE for general GCMs (i.e. with positive and negative multipliers) remains to be rigorously determined. At the light of our results, even the mere existence of a unique scaling law for $\lambda(N)$ turns out to be uncertain.

II. GLOBALLY COUPLED MAPS

The dynamics of a population of N globally coupled one-dimensional maps is iteratively governed by

$$y_i^{t+1} = f\left((1-\epsilon)\, y_i^t + \epsilon \bar{y}^t\right), \tag{3}$$

where the index $i \in \{1, \ldots, N\}$ labels the i-th map and $\bar{y}^t \equiv N^{-1}\sum_{j=1}^N y_j^t$ yields the all-to-all coupling. Here t is a discrete index for time. For each map, y_i is a scalar variable and the nonlinear function f defines the map. f is chosen such that yields chaotic dynamics for the uncoupled maps ($\epsilon = 0$). For small values of the all-to-all coupling ϵ the GCM (3) displays a fully turbulent phase [8] with N positive Lyapunov exponents.

To calculate the LE Eq. (3) is linearized, thereby obtaining the mapping rule for infinitesimal perturbations, $v_i^t \equiv \delta y_i^t$:

$$v_i^{t+1} = f'\left((1-\epsilon) y_i^t + \epsilon \bar{y}^t\right) \times \left[(1-\epsilon)\, v_i^t + \epsilon \bar{v}^t\right] \tag{4}$$

where f' stands for the derivative of f, and $\bar{v}^t \equiv N^{-1}\sum_{j=1}^N v_j^t$. The time- and site-dependent factors f' are

* Author to whom correspondence should be addressed; pazo@ifca.unican.es

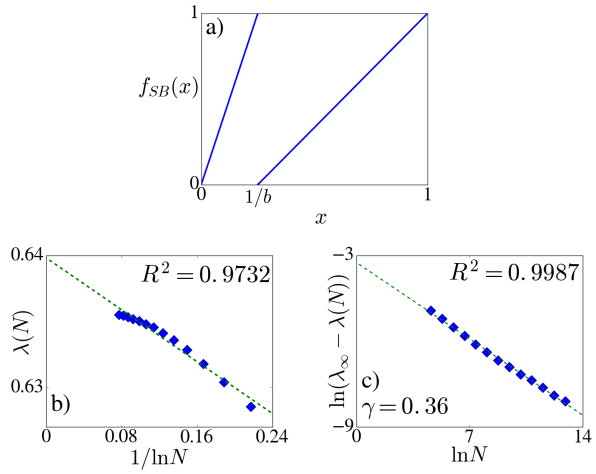

FIG. 1. (a) Skewed-Bernoulli map (6) with $b = 4$. (b,c) Two alternative forms of representing the LE of the SB-GCM as a function of the system size N, see x-axis. Parameters are $\epsilon = 0.02$, $b = 4$, and the largest size is $N = 409600$. The goodness of the linear fittings is indicated in each panel by the regression coefficient R^2.

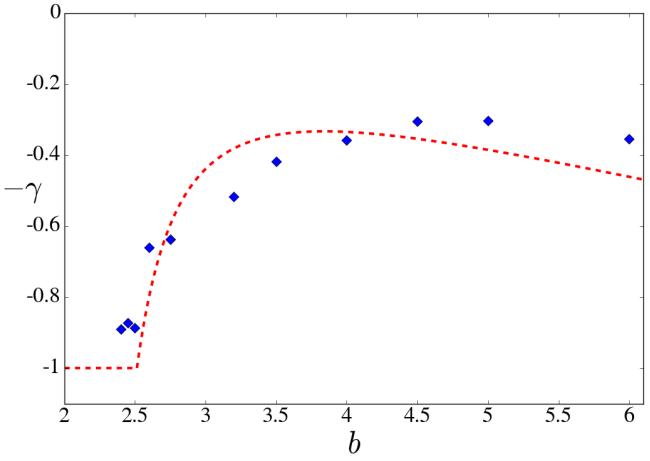

FIG. 2. Empirical values of the exponent $-\gamma$ for the SB-GCM as a function of the map parameter b. The coupling constant is fixed at $\epsilon = 0.02$. The red dashed line corresponds to the theoretical result for the RM model with bi-delta multipliers and the same parameter values.

hereafter referred to as the multipliers of the tangent dynamics. As time evolves, an arbitrary initial N-vector $\boldsymbol{v}^0 = (v_1^0, \ldots, v_N^0)$ converges to a statistically stationary configuration $\boldsymbol{v}^t$, called the Lyapunov vector.

The LE is a scalar quantity that characterizes the average exponential growth rate of infinitesimal perturbations: $\lambda = \lim_{t\to\infty} \frac{1}{t} \ln \|\boldsymbol{v}^t\|$. We may also obtain λ averaging the instantaneous logarithmic growth rate of the Lyapunov vector:

$$\lambda = \left\langle \ln \left(\frac{\|\boldsymbol{v}^{t+1}\|}{\|\boldsymbol{v}^t\|} \right) \right\rangle . \tag{5}$$

The bracket denotes the average over an infinite trajectory. According to the multiplicative Oseledets theorem [17, 18], the value of λ is (with probability one) the same for all initial perturbations $\boldsymbol{v}^{t=0}$, and all orbits starting in the basin of attraction of the chaotic attractor, provided the system is ergodic. Moreover, λ is an invariant that does not depend on the coordinate system nor on the specific norm type used in (5).

In general the Lyapunov vector components may fluctuate between positive and negative signs. However, if f' takes only positive values, then all the Lyapunov vector components have the same sign (in other words, this is an absorbing configuration).

III. PRELIMINARY NUMERICAL EVIDENCE

As a prototype of map with positive f' (multipliers) we choose the skewed-Bernoulli (SB) map:

$$f_{SB}(x) = \begin{cases} b\,x & \text{if } 0 \le x \le \dfrac{1}{b} \\ \dfrac{bx-1}{b-1} & \text{if } \dfrac{1}{b} < x \le 1 \end{cases} \tag{6}$$

Parameter b controls the chaoticity of the map. Figure 1(a) shows $f_{SB}(x)$ for parameter $b = 4$. The LE of a single uncoupled map depends on b as $\lambda_1 = \ln b - (1 - 1/b)\ln(b-1)$, which takes the reference value $\lambda_1 = 0.5623\ldots$ for $b = 4$. We adopt $b > 2$, since for $b = 2$ (skewness-free case) the dynamics is trivially chaotic with no intermittency.

Hereafter, the GCM made up of SB maps is referred to as SB-GCM for abbreviation. The coupling constant ϵ in Eq. (3) is chosen small, as this ensures a fully turbulent dynamics. The reference value $\epsilon = 0.02$ was selected in [7] and in Chap. 11 of [17]. The numerical value of the LE for the SB-GCM with $(b, \epsilon) = (4, 0.02)$ and different system sizes is represented in Figs. 1(b) and 1(c). In each plot a different scaling with N is assumed. In Fig. 1(b) we represent $1/\ln N$ in the x-axis, and a linear fit yields λ_∞ and the slope $-c$. For comparison in Fig. 1(c) a power-law scaling of the LE, see Eq. (2), is assumed instead, such that the data are fitted to a straight line in log-log scale: $\ln[\lambda_\infty - \lambda(N)] = k - \gamma \ln N$. Our strategy was to determine what value of λ_∞ yields an optimal linear fit to our data. For the particular choice of the coupling strength $\epsilon = 0.02$ and $b = 4$ we obtain $\gamma = 0.36$. The fitting is apparently superior with the power law than with the logarithmic law. However, in the former case we have three fitting parameters instead of two.

In order to increase the numerical evidence we measured the LE for several values of b (fixing $\epsilon = 0.02$) and determined the exponent γ following the procedure outlined above. Figure 2 shows the measured value of γ as a function of b. A significant variation in the value of γ is apparent. The main goal of this paper is ascertain the power-law convergence of $\lambda(N)$ to λ_∞, and explain the dependence of the exponent γ on parameters.

IV. MAIN RESULTS

Before presenting our theoretical results, and more numerical simulations, it is convenient to anticipate which are the main results of this paper. In [7] the logarithmic law (1) was linked to the power-law tail of the distribution of Lyapunov vector components. More specifically, in the thermodynamic limit the decay was claimed to be an inverse square law: $P(v \gg 1) \simeq c/v^2$. Here, in contrast, we find that the tail can obey a more general expression: $P(v \gg 1) \simeq c/v^{1+\alpha}$, where the tail index α depends on the model parameters. We distinguish three different regimes —labeled I, II and III—, in which the convergence of the LE to λ_∞ is different:

1. A first regime (I) with $\alpha \geq 2$ in which, the LE exhibits a robust power law, given by Eq. (2) with exponent $\gamma = 1$.

2. A second regime (II) in which $1 < \alpha < 2$ and the exponent γ varies in the range (0,1) with a smooth dependence on the parameters.

3. A third regime (III), which is only present when the values of the multipliers are very broadly distributed. This regime is much more complicated to analyze in detail, as α takes the value 1 (or smaller). This fact renders the analysis much more cumbersome and the main properties of this regime remain, in spite of our efforts, largely unknown. Our numerical simulations are consistent with a generalized logarithmic scaling $\lambda_\infty - \lambda(N) \simeq (\ln N)^{-\delta}$, but we must be cautions upon drawing general conclusions in this case.

V. RANDOM MULTIPLIER MODEL

Given that direct numerical results with GCMs will be always inconclusive, we turn our view to a minimal model that can be theoretically analyzed. This is a stochastic model of the tangent-space dynamics of GCMs proposed in Ref. [7]. The model simply replaces the local multipliers f' in Eq. (4) by independent identically distributed random numbers μ_i^t. Hence we have

$$v_i^{t+1} = \mu_i^t \left[(1-\epsilon)v_i^t + \epsilon \bar{v}^t\right]. \tag{7}$$

Note that ignoring correlations between the multipliers is tantamount to ignoring the collective dynamics of the mean field $\bar{y}^t$ present in actual GCMs. As in [7], we assume weak correlations induced by the collective dynamics do not alter the final result. Our analytical results are entirely based on the random multiplier (RM) model (7).

Before starting the analysis of (7), we briefly introduce the three multiplier densities used to assess the validity of our results. Our first case study is the bi-delta density:

$$\rho_{BD}(\mu) = \frac{1}{b}\delta(\mu - b) + \frac{b-1}{b}\delta[\mu - b/(b-1)]. \tag{8}$$

This form for $\rho(\mu)$ corresponds to the binary occurrence of f' for an unperturbed SB map with parameter b.

The second example is the log-normal distribution:

$$\rho_{LN}(\mu) = \frac{1}{\sqrt{2\pi}a\mu} e^{-(\ln \mu)^2/(2a^2)}. \tag{9}$$

This distribution was originally considered in [7] for the absolute value of the multiplier $|\mu|$. It is implemented by taking the exponential of uncorrelated zero-mean Gaussian random variables ξ_j^t: $\mu_j^t = \exp(\xi_j^t)$. The variance of ξ_j^t being a^2.

The last case study is the log-uniform distribution, in which the multipliers are chosen as the exponential of a uniform random variable in the interval $[-m, m]$. The multiplier density in this case has the form

$$\rho_{LU}(\mu) = \begin{cases} \frac{1}{2m\mu} & \text{if } e^{-m} < \mu < e^m \\ 0 & \text{otherwise} \end{cases} \tag{10}$$

VI. THE ASYMPTOTIC LYAPUNOV EXPONENT λ_∞

Restricting to positive multipliers allows us to obtain analytical expressions for the LE. First, we average both sides of Eq. (7):

$$\bar{v}^{t+1} = (1-\epsilon)\overline{\mu v}^t + \epsilon \bar{\mu}^t \bar{v}^t, \tag{11}$$

where $\overline{\mu v}^t \equiv N^{-1}\sum_{j=1}^N \mu_j^t v_j^t$. The positiveness of the vector components makes their average equal to the taxicab norm; or more formally, $\bar{v}^t = \|\boldsymbol{v}^t\|_1 = (1/N)\sum_{i=1}^N v_i^t$. From Eq. (11) we obtain the ratio between consecutive perturbation averages:

$$\frac{\bar{v}^{t+1}}{\bar{v}^t} = \bar{\mu}^t \left[\epsilon + (1-\epsilon)\frac{\overline{\mu v}^t}{\bar{\mu}^t \bar{v}^t}\right], \tag{12}$$

and, according to Eq. (5), the LE equals the average of the logarithm of the above formula:

$$\lambda(N) = \left\langle \ln \bar{\mu}^t \right\rangle + \left\langle \ln \left[\epsilon + (1-\epsilon)\frac{\overline{\mu v}^t}{\bar{\mu}^t \bar{v}^t}\right] \right\rangle. \tag{13}$$

We wish to determine here the value of the LE in the thermodynamic limit $\lambda_\infty = \lambda(N \to \infty)$. Of the two terms contributing to $\lambda(N)$ in Eq. (13), the first one is trivial since the sample average of the multipliers converges to its mean: $\lim_{N\to\infty} \bar{\mu}^t = \langle \mu \rangle$. To recognize the asymptotic behavior of

$$s^t \equiv \frac{\overline{\mu v}^t}{\bar{\mu}^t \bar{v}^t} \tag{14}$$

in Eq. (13) is crucial to complete the result.

As a preliminary step we prove first that the expected value of s^t equals 1, just assuming the all the Lyapunov vector components are statistically equivalent. First, we rewrite $s^t = \sum_j \tilde{\mu}_j^t v_j^t / (\sum v_j^t)$, where $\tilde{\mu}_j^t = \mu_j^t / \bar{\mu}^t$. Now the expected value of s is

$$\langle s^t \rangle = \left\langle \frac{\sum_j \tilde{\mu}_j^t v_j^t}{\sum_j v_j^t} \right\rangle = \left\langle \sum_{j=1}^N \tilde{\mu}_j^t v_j^t \right\rangle = \sum_{j=1}^N \left\langle \tilde{\mu}_j^t \right\rangle \left\langle v_j^t \right\rangle = 1, \tag{15}$$

where we have chosen the normalization $\sum_j v_j^t = 1$ in the second equality, used the independence of $\tilde{\mu}_j$ and v_j^t, and substituted $\langle \tilde{\mu}_j^t \rangle$ and $\langle v_j^t \rangle$ by 1 and $1/N$, respectively. Now, we consider the thermodynamic limit of Eq. (13). Due to the convexity of the logarithm, the expected value of $\ln[\epsilon + (1-\epsilon)s^t]$ is not larger than $\ln[\epsilon + (1-\epsilon)\langle s^t \rangle]$, we obtain that

$$\lambda_\infty \leq \ln\langle \mu \rangle. \tag{16}$$

The previous constraint turns into an equality with a few additional assumptions. Let us assume that, given a certain norm (e.g. $\bar{v} = 1$), each Lyapunov vector component is uncorrelated from the rest and it is drawn from a stationary probability density $P_s(v)$. If such a $P_s(v)$ really exists is discussed later on. As the multipliers and the vector components are uncorrelated, we have a quite robust trivial result: $\lim_{N\to\infty} s^t = 1$, provided the expected value of v exists, see e.g. [19]. We get thus the simple relation:

$$\lambda_\infty = \ln\langle \mu \rangle. \tag{17}$$

This value of λ_∞ is larger than $\lambda_1 = \langle \ln \mu \rangle$, the LE for a single uncoupled map. This means that an extreme 'coupling sensitivity of chaos' [20] shows up in the thermodynamic limit. The identity in Eq. (17) is valuable for the numerical validation of the theory with the RM model since λ_∞ is not a fitting parameter anymore (in contradistinction to the general case of GCMs).

VII. THE LYAPUNOV VECTOR AND ITS LOCALIZATION

Before addressing our main question (i.e., the size dependence of the LE), it is necessary to suitably describe the Lyapunov vector in the thermodynamic limit ($N \to \infty$). Indeed, as shown later, the localization strength of the Lyapunov vector is intimately related with the convergence of the LE with N.

First of all, we note that in the thermodynamic limit Lyapunov vector components are expected to be distributed as a stationary density if the exponential amplification is removed [17]: $P(v,t) = P(v\, e^{-\lambda_\infty t}, 0)$ [21]. The norm of the Lyapunov vector is irrelevant as it can always be scaled out. Hence we only need $P(v,0) = P_s(v)$. Takeuchi et al. [7] addressed the problem resorting to a Hopf-Cole transformation and then solving the stationary solution of Fokker-Planck equation. We replicate part of their mathematical treatment in the following lines. We note, however, that the conclusions of our analysis are radically different.

First of all, we make the Hopf-Cole transformation of the vector components:

$$u_i^t = \ln v_i^t. \tag{18}$$

As we are assuming positive multipliers $\mu_j^t > 0$, the v_i^t remain above zero at all times, hence no absolute value is required to take the logarithm [22].

In terms of the u variables the evolution equation of the RM model (7) becomes:

$$u_j^{t+1} = u_j^t + \ln \mu_j^t + \ln(1-\epsilon) + \ln\left(1 + \frac{\epsilon \bar{v}^t e^{-u_j^t}}{1-\epsilon}\right). \tag{19}$$

For simplicity of notation, we keep $\bar{v}^t$ instead of writing $\overline{e^u}^t$.

Replacing a discrete difference in time by a time derivative, the corresponding Fokker-Planck equation for the density $\tilde{P}(u,t)$ in the co-moving reference frame at velocity λ_∞ is

$$\partial_t \tilde{P}(u,t) = -\partial_u[(\lambda_0(u) - \lambda_\infty)\tilde{P}(u,t)] + \frac{D}{2}\partial_{uu}\tilde{P}(u,t), \tag{20}$$

where

$$\lambda_0(u) = \langle \ln \mu \rangle + \ln(1-\epsilon) + \ln\left(1 + \frac{\epsilon \bar{v} e^{-u}}{1-\epsilon}\right), \tag{21}$$

and the constant D is the variance of the noise, which is given by

$$D = \mathrm{var}(\ln \mu) \tag{22}$$

If the constant λ_∞ is the LE in the limit $N \to \infty$, a stationary solution, $\tilde{P}_s(u)$, of (20) exists and is given by the solution of

$$\frac{d}{du}[(\lambda_\infty - \lambda_0(u))\tilde{P}_s(u)] + \frac{D}{2}\frac{d^2}{du^2}\tilde{P}_s(u) = 0. \tag{23}$$

We do not need the exact solution of this equation, only the asymptotic (large u) decay of $\tilde{P}_s(u)$ will be of our interest. The solution of (23) exhibits an exponential decay:

$$\tilde{P}_s(u \to \infty) \simeq k\, e^{-\alpha u}, \tag{24}$$

where $\alpha = 2[\lambda_\infty - \lambda_0(u \to \infty)]/D$ measures the Lyapunov vector localization strength. Recalling Eqs. (21) and (22) we can express α in terms of ϵ and the statistical properties of μ:

$$\alpha = 2\,\frac{\lambda_\infty - \langle \ln \mu \rangle - \ln(1-\epsilon)}{\mathrm{var}(\ln \mu)}. \tag{25}$$

This formula relates the Lyapunov vector localization index α with λ_∞, the multiplier density, and the coupling strength ϵ. As intuitively expected α grows with ϵ, i.e., the vector becomes less localized as the coupling is increased.

Moreover, as we already know λ_∞, via Eq. (17), the value of exponent α in Eq. (25) becomes completely determined:

$$\alpha = 2\,\frac{\ln\langle \mu \rangle - \langle \ln \mu \rangle - \ln(1-\epsilon)}{\mathrm{var}(\ln \mu)}. \tag{26}$$

This formula relates the localization strength of the Lyapunov vector, i.e. its tail index α, with known quantities. As a numerical check, the empirical $\tilde{P}_s(u)$ is represented in Fig. 3 for specific parameters of the RM model with bi-delta multiplier density. The observed decay rate at large u is in good agreement with the result of Eq. (26): $\alpha = 1.44$. The asymptotic

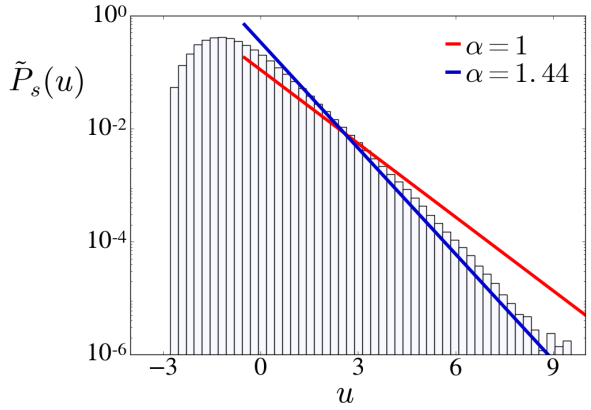

FIG. 3. Probability density $\tilde{P}_s(u)$ obtained form numerical simulations of the RM model with bi-delta density (8) and parameters $\epsilon = 0.02$, $b = 3$. The system size is $N = 409600$, and the components of the Lyapunov vector were retrieved at 100 different times, fixing $\bar{v} = 1$, to estimate $\tilde{P}_s(u)$. The straight lines correspond to the exponential $\propto e^{-\alpha u}$, with $\alpha = 1$ (red), as predicted in [7], and $\alpha = 1.44$ (blue), as obtained from our theory in Eq. (26), see also Table I.

slope predicted by Takeuchi et al. is -2 (i.e., $\alpha = 1$), which is in clear disagreement with the data.

Reverting the Hopf-Cole transformation in (18), Eq. (24) translates into a power-law tail of the stationary density of the vector components:

$$P_s(v \to \infty) \simeq k'\, v^{-1-\alpha}. \tag{27}$$

We can go one step forward and use Eq. (26) to generate phase diagrams for the three multiplier probability distribution types introduced in Sec. V. In Fig. 4 we show the phase diagrams for the bi-delta, log-normal, and log-uniform multiplier densities in panels (a), (b) and (c), respectively. The ranges of ϵ depicted in Fig. 4 can be particularly large since the RM model is always representing the turbulent regime. In actual GCMs, turbulence typically ceases to exist already for $\epsilon \sim 0.1$.

The level lines $\alpha = 2$ and $\alpha = 1$ are specially interesting, as they mark the boundaries between different regimes, depending on the statistical properties of the random multipliers and coupling strength. In particular, the line $\alpha = 2$, Fig. 4(c), is the boundary that separates models for which the probability density of vector components, $P_s(v)$, exhibits a finite variance from those where it does not. The effect of model parameters on the asymptotic scaling properties of the LE with the system size will be analyzed in detail in Sec. VIII.

The existence of these boundary lines depends on the random multipliers specific statistics. Note, for instance, that the level line $\alpha = 1$, does not exist for the bi-delta multiplier distribution, and coincides with $\epsilon = 0$ for the log-normal distribution (see Figs. 4(a) and 4(b)). However, for the log-uniform multiplier distribution this line is indeed present at finite ϵ values, see Fig. 4(c). We stress here that, in the green shaded region, Fig. 4(c), our previous theory breaks down, since it predicts $\alpha < 1$. This possibility is forbidden because for any finite population, such a density leads to a paradoxical result, as we explain in the following. In a finite population we can fix $\bar{v} = 1$, and the largest component v_{max} cannot be larger than N. However, if one draws the vector components from a density with a tail decaying as $v^{-1-\alpha}$ inconsistencies arise. The probability for one vector component being larger than N is $\Pr(v > v_{max} = N) = \int_N^\infty P_s(v)dv \sim N^{-\alpha}$; and the probability all components are below N is roughly $(1 - N^{-\alpha})^N \simeq 1 - N^{1-\alpha}$, which approaches 1 if $\alpha > 1$. If $\alpha < 1$, some components will exceed the largest allowed value $v_{max} = N$ almost surely as N grows. In the marginal case $\alpha = 1$, the situation is exactly at the edge.

In the next section we analyze the regular case, $\alpha > 1$, and derive a power-law convergence for the LE. The study of the anomalous green region in Fig. 4(c), is postponed to Sec. IX.

VIII. REGIMES I AND II: POWER-LAW CONVERGENCE OF THE LYAPUNOV EXPONENT

The convergence of the LE to λ_∞ whenever $\alpha > 1$ is analyzed next, performing a perturbation expansion of Eq. (13). We start replacing all $\bar{\mu}^t$ by $\langle\mu\rangle$ in Eq. (13). This approximation is sensible provided that the multipliers are not fat-tailed distributed, what we forbid. Time fluctuations of $\bar{\mu}^t$ yield deviations of order N^{-1}, e.g. $\ln\bar{\mu}^t \simeq \ln\langle\mu\rangle + O(N^{-1})$. These $O(N^{-1})$ terms can be safely neglected, as the convergence of $\lambda(N)$ to λ_∞ is dominated by the statistics of the vector components as verified *a posteriori*. Keeping in mind that terms of order $O(N^{-1})$ are neglected, Eq. (13) yields the approximation

$$\lambda(N) \simeq \lambda_\infty + \left\langle \ln\left[\epsilon + (1-\epsilon)s^t\right]\right\rangle. \tag{28}$$

Now, given that $\lim_{N\to\infty} s^t = 1$ and $\langle s^t\rangle = 1$, we Taylor expand the logarithm up to second order:

$$\lambda_\infty - \lambda(N) \simeq \frac{(1-\epsilon)^2}{2}\mathrm{var}(s^t). \tag{29}$$

To proceed further with the calculation we can resort to Eq. (3) in Ref. [19]. Nevertheless, the interested reader can find the detailed calculation in the Appendix. The final result for the leading order correction to λ_∞ is:

$$\lambda_\infty - \lambda(N) \simeq \frac{(1-\epsilon)^2\mathrm{var}(\mu)}{2\langle\mu\rangle^2}\left\langle \frac{\sum_{j=1}^N (v_j^t)^2}{\left(\sum_{j=1}^N v_j^t\right)^2}\right\rangle. \tag{30}$$

In the Appendix the goodness of the approximations are tested for the bi-modal multiplier density. Unfortunately, even for moderate values of b, say above 4, to achieve the asymptotic regime is computationally too demanding for our current numerical capabilities.

With Eq. (30) the problem reduces to properly estimate the average in the right hand side. Writing that equation in this form:

$$\lambda_\infty - \lambda(N) \simeq \frac{(1-\epsilon)^2\mathrm{var}(\mu)}{2\langle\mu\rangle^2 N}\left\langle \frac{\overline{v^2}^t}{(\bar{v}^t)^2}\right\rangle, \tag{31}$$

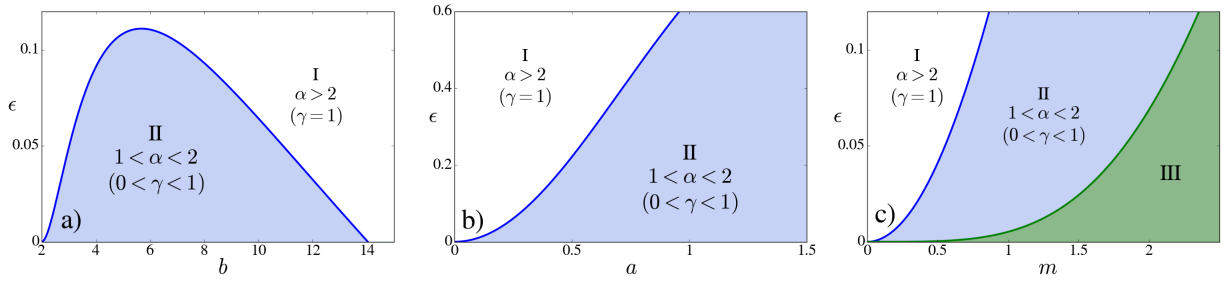

FIG. 4. Phase diagrams of the RM model for three multiplier densities: (a) Bi-delta, Eq. (8); (b) Log-normal, Eq. (9); (c) Log-uniform, Eq. (10). Level lines of $\alpha = 1, 2$, obtained from Eq. (26), enclose regimes I, II and III.

TABLE I. Statistical properties of the three multiplier probability density types we study in this paper. The last column is the theoretical prediction for the tail index α describing the asymptotic decay of the Lyapunov vector components distribution for each RM model, according to Eq. (26). (*) In the case of the log-uniform density the result is valid only for $\alpha > 1$.

Density $\rho(\mu)$	$\lambda_\infty = \ln\langle\mu\rangle$	$\langle \ln \mu\rangle$	$\mathrm{var}(\ln\mu)$	Tail index* α
Bi-delta, Eq. (8)	$\ln 2$	$\frac{1}{b}\ln b + \frac{b-1}{b}\ln\left(\frac{b}{b-1}\right)$	$\frac{(b-1)\ln^2(b-1)}{b^2}$	$\frac{2b\left[b\ln\left(\frac{2}{1-\epsilon}\right)-(b-1)\ln\left(\frac{b}{b-1}\right)-\ln b\right]}{(b-1)\ln^2(b-1)}$
Log-normal, Eq. (9)	$\frac{a^2}{2}$	0	a^2	$1-\frac{2\ln(1-\epsilon)}{a^2}$
Log-uniform, Eq. (10)	$\ln\left(\frac{\sinh m}{m}\right)$	0	$\frac{m^2}{3}$	$\frac{6\left[\ln\left(\frac{\sinh m}{m}\right)-\ln(1-\epsilon)\right]}{m^2}$

it becomes apparent that the expected convergence rate of the LE would be N^{-1} if the Lyapunov vector was completely delocalized, i.e., all components taking comparable values on average. However this is not the case because, as seen above, the components of the Lyapunov vector are distributed with a power-law tail (in the thermodynamic limit). Therefore, we must examine the average in Eq. (30) more carefully.

A. Exponent γ

Actually, calculating the average

$$T_N \equiv \left\langle \frac{\sum_{j=1}^N (v_j^t)^2}{\left(\sum_{j=1}^N v_j^t\right)^2} \right\rangle \tag{32}$$

that appears in Eq. (30) turns out to be a formidable task. We have N non-independent Lyapunov vector components evolving in time. To proceed further we assume that the distribution of v in the thermodynamic limit is all we need to estimate Eq. (32) at leading order. Correlations originating from the finiteness of the population are regarded as higher-order effects, which we shall ignore within our approximation. Thus, we assume vector components v_j are independent (identically distributed) random variables. Under this natural assumption analytical results are available in the mathematical literature. For distributions with a Pareto-type decay and tail index α, i.e. Eq. (27), the asymptotic dependence of T_N on N is analytically known to scale as [23, 24]:

$$T_N \sim \begin{cases} \Gamma(2-\alpha)\ell(N)N^{1-\alpha} & \text{for } 1<\alpha<2 \\ \langle v^2\rangle N^{-1} & \text{for } \alpha > 2 \end{cases} \tag{33}$$

Here $\ell(N)$ is a "slowly varying function" satisfying $\lim_{N\to\infty}\ell(N)/\ln(N) = 0$, and we have fixed $\langle v\rangle = 1$ to make the expressions less convoluted. According to Eq. (33), the statistic T_N decays as a power of N for all α values, and so does $\lambda_\infty - \lambda(N)$ by virtue of Eq. (30). Specifically, if $\alpha > 2$, the probability $P_s(v)$ in Eq. (27) has finite variance and the trivial exponent, corresponding to a delocalized vector, is immediately recovered. In contrast, if $1 < \alpha < 2$ the exponent adopts a nontrivial value: $\gamma = \alpha - 1$. For the sake of clarity, we find it convenient to cast these results into a single expression:

$$\gamma_{i.i.d.} = \min(\alpha - 1, 1), \tag{34}$$

where $\alpha > 1$ has a known dependence on the distribution of the multipliers given by our theory through Eq. (26). The subscript $i.i.d.$ indicates that the hypothesis of independent vector components is assumed. Remarkably, the stronger the localization of the Lyapunov vector the slower the convergence of the Lyapunov exponent, i.e. $\gamma \to 0^+$ as $\alpha \to 1^+$.

Here concludes the proof of our main result in Eq. (2), supplemented by Eqs. (34) and (26). The correctness of our prediction for the exponent γ relies on the validity of the assumption of complete independence of the vector components. This is a reasonable approximation, albeit not fully justified. Nonetheless, the main result summarized in the power law in Eq. (2) is probably quite robust. For comparison, let us mention that the behavior of T_N when the v_j's are drawn in a deterministic way —selecting values at which the cumulative distribution function equals $(j-1)/N$— is also a power law with a slightly different exponent [23]: $\gamma_{\rm det} = \min(2 - 2/\alpha, 1)$. As $\gamma_{i.i.d.}$, also $\gamma_{\rm det}$ equals 1 for $\alpha \geq 2$ and vanishes as $\alpha \to 1$. The difference between $\gamma_{\rm det}$

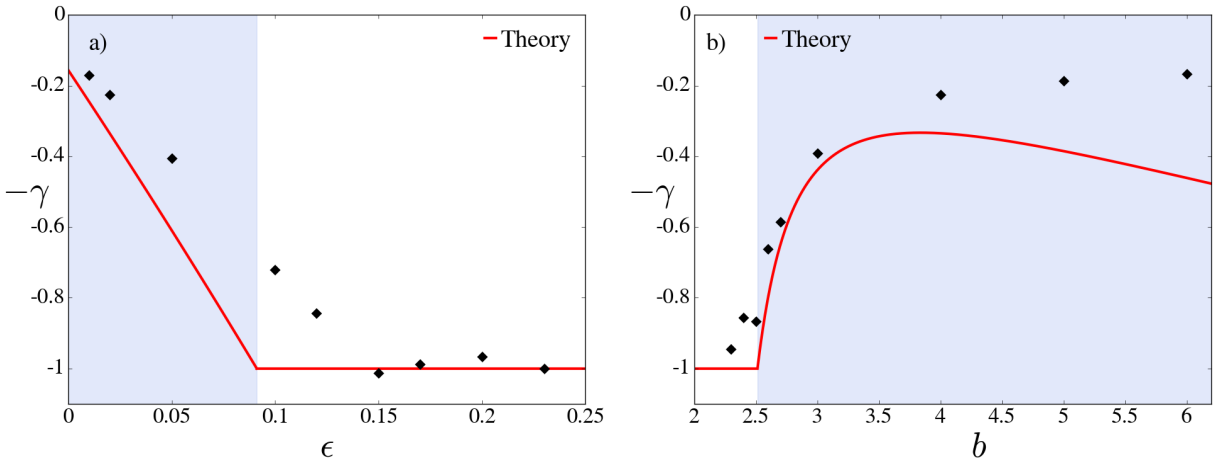

FIG. 5. RM with bi-delta density. Numerical estimate of the power-law exponent $-\gamma$ and comparison with the theory, Eqs. (26), and (34), see also Table I for $b = 4$ in (a), and $\epsilon = 0.02$ in (b). The background shading in both panels indicates parameter values inside region II of Fig. 4(a).

and $\gamma_{i.i.d.}$ is no more than 0.17 (the maximum difference is achieved at $\alpha = \sqrt{2}$). Expressing some caution, we believe this may give an idea of the degree of accuracy of the results based upon the $i.i.d.$ hypothesis above.

B. Numerical results

In this section we test the validity of our results for the RM model with the three multipliers density types summarized in Table I. Actually, a thorough numerical verification of the predicted phase diagrams in Fig. 4 is far too demanding. Alternatively, we can determine numerically the exponent γ along selected sections of the phase diagrams. For specific parameter values, $\lambda(N)$ is measured for several system sizes (up to $N = 409600$), and the value of $-\gamma$ is the slope obtained from the linear fit $\ln[\lambda_\infty - \lambda(N)] = k - \gamma \ln N$, where λ_∞ is known to be $\ln\langle\mu\rangle$.

1. *Bi-delta multiplier density*

Irrespective of the particular values of b and ϵ, the Lyapunov exponent converges to $\lambda_\infty = \ln\langle\mu\rangle = \ln 2$. In Figs. 5(a) and 5(b), the numerical estimations of $-\gamma$ are represented at fixed b and fixed ϵ, respectively. For comparison, the theoretical prediction of γ, via Eq. (34), and the α value in Table I are plotted as solid lines. As can be seen in both panels of Fig. 5, the exponent γ strongly depends on parameters. In panel (a) the elbow at $\epsilon \approx 0.09$ is not accurately captured by the data, but the general behavior of γ is successfully reproduced. In Fig. 5(b), γ significantly departs from the theory as b grows above 4. This is not surprising, as our numerical tests— see Fig. 12 in the Appendix— already revealed the slow convergence to the asymptotic regime for moderate b values. In any case Fig. 5(b) exhibits a trend of γ similar to the SB-GCM in Fig. 2 with the same ϵ value. In our view, this confirms the validity our analysis.

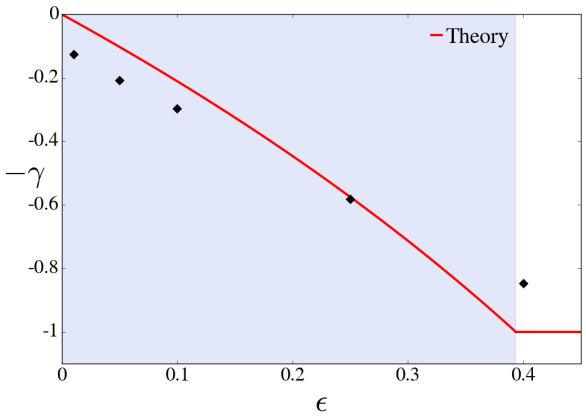

FIG. 6. RM model with log-normal density with $a = 1$. Numerical determination of the exponent γ as the coupling ϵ is varied and comparison with our theoretical prediction.

2. *Log-normal multiplier density*

In Fig. 6, we monitor γ as a function of the coupling parameter for $a = 1$. The numerical results and theory are in reasonable agreement, in our opinion, and the general trend of γ is fairly reproduced. As a side note, we point out that including the exact value of $\lambda_\infty = \ln\langle\mu\rangle$ in the fittings is crucial. The actual values of the multipliers are affected by the accuracy of the Gaussian random number generator, such that the difference between the numerical value of $\ln\langle\mu\rangle$ and the expected value $a^2/2 = 1/2$ is of the order of 10^{-3}.

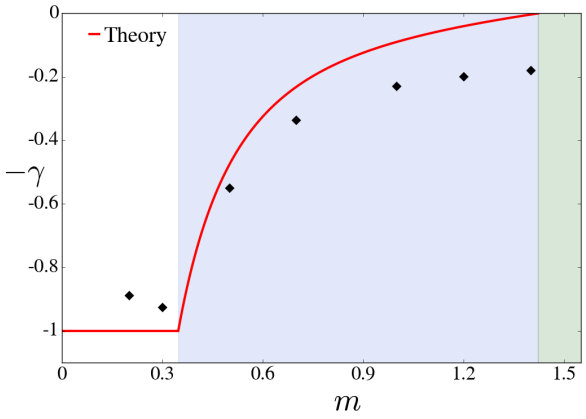

FIG. 7. RM model with log-uniform density. Numerical results for the exponent γ as a function of parameter m for a coupling strength $\epsilon = 0.02$. The background shading indicates parameter values inside regions II (blue) and III (green) of Fig. 4(c).

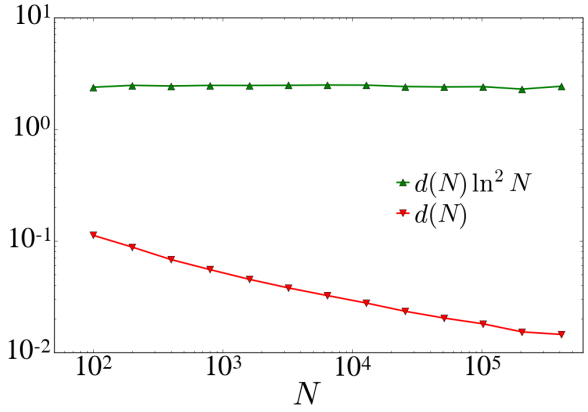

FIG. 8. Numerical results for the diffusion coefficient defined by Eq. (36) as a function of N for the RM model with log-uniform multiplier density and parameters $\epsilon = 0.02$ and $m = 2$.

3. *Log-uniform multiplier density*

Figure 7 shows the empirical values of γ as a function of m for $\epsilon = 0.02$. As m grows, the values of the random multipliers become increasingly scattered and, as already discussed, the boundary of the power-law behavior (corresponding to $\alpha = 1$) is located at the critical value $m_c = 1.422\ldots$. As anticipated, strong finite-size effects in the simulations hinder the convergence of γ to zero, as m approaches m_c. Said that, we estimate the theory works reasonably well, given the complexity of the problem.

IX. REGIME III

The goal of describing the Lyapunov dynamics in regime III requires a non trivial refinement of our theory. We advance that theoretical and computational obstacles have not allowed us to accomplish that goal so far. Nonetheless, it may be instructive to devote this section to enumerate the main difficulties we have encountered, and to discuss some partial results.

In contrast to regions I and II, in region III the components of the Lyapunov vector are strongly scattered, such that the limit v_{max} proportional to N cannot be ignored. Roughly speaking, the finiteness of the system is always relevant, and it is not even obvious if a density $P_s(v)$ is meaningful in the thermodynamic limit.

A. Vanishing diffusion coefficient

In order to confirm that the chaotic dynamics is self-averaging in the thermodynamic limit we computed the diffusion coefficient, characterizing the intermittency of chaos [17, 25]. Before introducing our numerical results we briefly summarize a few basic notions. Let $\lambda(\tau, t_0; N)$ be the finite-time Lyapunov exponent of a system of size N.

$$\lambda(\tau, t_0; N) = \frac{1}{\tau} \ln \frac{\bar{v}^{t_0+\tau}}{\bar{v}^{t_0}}. \tag{35}$$

This quantity depends on the time interval τ, and on the state of the system through t_0. The LE is recovered in the limit $\lambda(N) = \lim_{\tau\to\infty} \lambda(\tau, t_0; N)$. The diffusion coefficient d is an invariant that quantifies mean quadratic deviations from the average exponential growth of infinitesimal perturbations [17]:

$$d(N) = \lim_{\tau\to\infty} \frac{\left\langle (\lambda(\tau, t_0; N)\tau - \lambda(N)\tau)^2 \right\rangle}{\tau} \tag{36}$$

In a generic chaotic system d is nonzero. In our RM model, d departs from zero, due to the fluctuations of the FTLE caused by $\bar{\mu}^t$ and s^t, see Eq. (13). To ascertain whether this fluctuation persists in the thermodynamic limit, we computed $d(N)$ for several system sizes and fixed parameter values well inside region III ($m = 2$ and $\epsilon = 0.02$). The numerical result in Fig. 8 shows that the decay of $d(N)$ to zero is consistent with the inverse of the logarithm squared: $d(N) \simeq c/\ln^2 N$. To our surprise, this decay is robust over several decades. The fact that $d(N \to \infty) \to 0$ implies that there exist a co-moving reference frame in which the Lyapunov vector is stationary in the thermodynamic limit.

B. The Lyapunov vector

In view that a stationary density $\tilde{P}_s(u)$ exists in the thermodynamic limit, we decided to measure it numerically for a large system size. In Fig. 9 we can see the distribution of the (log-transformed) vector components from an average over 50 states. Notably, the tail decays with a slope that gives approximately $\alpha = 0.85$, which is appreciably steeper than the prediction from Eq. (26): $\alpha = 0.7276\ldots$. As previously discussed, values of α below 1 eventually yield too large vector components, above the maximal allowed value $u_{max} = \ln N$

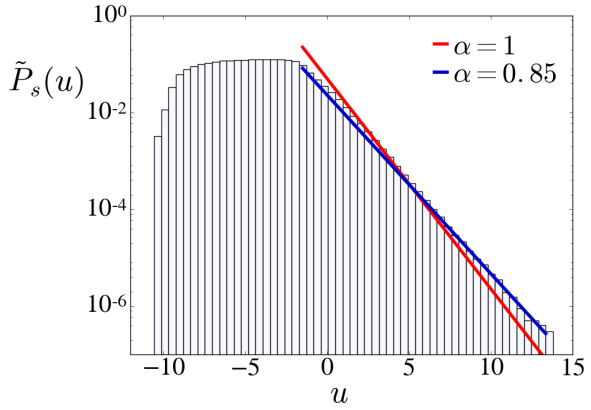

FIG. 9. Numerical probability distribution of log-transformed vector components $u_j = \ln v_j$ for the log-uniform RM model for a population of size $N = 2^{14} \times 100 \approx 1.6 \times 10^6$. Parameters are $m = 4$ and $\epsilon = 0.02$. The histogram is an average over 50 vector configurations with $\bar{v} = 1$. The red and blue straight lines are exponentials $\propto e^{-\alpha u}$ with $\alpha = 1$ and 0.85, respectively.

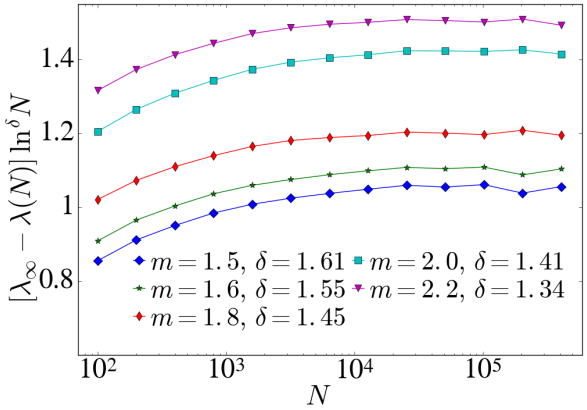

FIG. 10. Rescaled LE difference $[\lambda_\infty - \lambda(N)] \ln^\delta N$ for the log-uniform RM model with $\epsilon = 0.02$ and several values of the map parameter m. For each m value, a different value of δ seems to be required to reach a plateau at large N.

(for $\bar{v} = 1$). For the example, in Fig. 9 one can appreciate that the vector components are spread up to that limit: $u_{max} = 14.3\ldots$. We suspect that the slope progressively decreases as N grows, approaching to -1 in the thermodynamic limit. Another possibility is the existence of a prefactor in the power law density. With an abuse of language: $\tilde{P}_s(u) \sim f(N)e^{-\alpha u}$, with $f(N) \sim N^{-1+\alpha}$. An extensive and systematic numerical exploration might eventually clarify this issue.

C. Numerical exploration of the Lyapunov exponent

One important consequence of the decay to zero of the diffusion coefficient in regime III is that the constraint for λ_∞ in Eq. (16) becomes the identity in Eq. (17) (as in regimes I and II). The knowledge of $\lambda_\infty = \ln\langle\mu\rangle$ persuaded us to explore the dependence of $\lambda(N)$ numerically. Our guess is that the dependence must be logarithmic, as in the case of $d(N)$. For comparison, it is known that, in one-dimensional spatio-temporal extensive chaos, $\lambda(L)$ and $d(L)$ depend on the system size L algebraically as L^{-1} [4] and $L^{-1/2}$ [26, 27], respectively. By analogy, we attempted to accommodate our LE to a generalized logarithmic scaling

$$\lambda_\infty - \lambda(N) \simeq \frac{c}{\ln^\delta N} \tag{37}$$

Comparatively, our results in Fig. 10 are much less robust than those for $d(N)$ in Fig. 8. As the system size increases the effective exponent δ grows as well. We achieved systems sizes up to $N \approx 4 \times 10^5$ in Fig. 10. For each value of m, all of them in region III, a different value of δ flattens the curves at large N (notice the scaling with $\ln^\delta N$ in the y-axis). As previously mentioned, in all cases there is a systematic increase of δ as N grows. From our numerical results, we cannot discern if δ takes a common asymptotic value or not.

D. Rationale for a logarithmic law

The lack of diffusion in the thermodynamic limit, as well as a numerical check (not shown), indicates that s^t in Eq. (13) fluctuates around 1 with a decreasing amplitude as N grows. As before, this allows us expanding the logarithm in Eq. (28), and subsequently deriving the expression

$$\lambda_\infty - \lambda(N) \propto \mathrm{var}(\tilde{\mu}) T_N, \tag{38}$$

where T_N is given by Eq. (32), and $\tilde{\mu}$ was defined in Sec. VI. According to McLeish and O'Brien [23], $T_N \sim (\ln N)^{-1}$ if the tail index α equals unity. This dependence would propagate up to $\lambda(N)$. Note, however, that the result in [23] is fragile and breaks down under a change in the drawing rule of the vector components: If they are selected deterministically, then $T_N \sim (\ln N)^{-2}$. In the case of the Lyapunov vector, components are indeed not completely independent as the bound $v_j < N$ (if $\bar{v} = 1$) immediately introduces certain correlations. Should we expect a convergence as $(\ln N)^{-\delta}$ for the LE with $1 \leq \delta \leq 2$? Is the numerical value of δ unique, or varies with the parameters? Unfortunately, we cannot give a proper answer to these questions at this stage, and they are left as open problems.

X. DISCUSSION

A. Positive Multipliers: Regimes I, II, and III

Our theoretical findings, built upon the random multiplier model proposed by Takeuchi et al. [7], support the existence of three scaling regimes for turbulent GCMs with positive multipliers. This result immediately contradicts the very expectation of a unique universal scaling law for the LE for this problem. Regimes I and II exhibit power law behavior with different exponents. For regime III, however, we could not determine the actual scaling properties, although everything

indicates it converges slower than a power law. Having the exact value of λ_∞ allowed us to explore the conformity with a generalized logarithmic law, Eq. (37). But, clearly, more theoretical work is needed to better characterize GCMs in this regime.

B. Implications for the general case: Positive and negative multipliers

Our results do not apply to turbulent GCMs in which positive and negative multipliers participate in the tangent dynamics. Nonetheless, our work immediately reveals that part of the analysis in [7] is flawed. Let us enumerate, point-by-point, the key points leading us to this important conclusion:

1. The theoretical approximation in [7] does not require any condition on the sign of the multipliers. As already explained, the lack of sign-defined multipliers translates into Lyapunov-vector components with both signs. To cope with this, in [7], the Hopf-Cole transformation simply includes an absolute value: $u_i^t = \ln|v_i^t|$. Exclusively positive multipliers is a best-case scenario, since the Hopf-Cole transformation is invertible. If not, the problem is somehow brushed "under the carpet".

2. For positive multipliers the density of the Lyapunov vector components rapidly decays to 0 as $v \to 0$ (or as $u \to -\infty$), see Figs. 3 and 9. This is consistent with the asymptotic behavior of the stationary solution of the Fokker-Planck Eq. (23). After straightforward calculations we get: $\tilde{P}_s(u \to -\infty) \propto e^{-u^2/D}$ as $u \to -\infty$. This abrupt decay is perceived as a lower wall in the density. Such a lower wall is invoked by Takeuchi et al. [7], see also Chap. 11 of [17], although in their reasoning finite-N and infinite-N perspectives are intermingled. In deep contrast, if positive and negative multipliers exist there is no lower wall. In the empirical distribution shown in Fig. 11 for a particular case (see caption), we observe $\tilde{P}_s(u \to -\infty) \propto e^u$, implying $P_s(v \to 0) = \text{const}$. This is not consistent with the Fokker-Planck equation. The case of positive multipliers is, again, in better agreement with the ideas in [7].

3. In spite of the apparent validity of the Fokker-Planck equation (at least, for positive multipliers), the predicted logarithmic scaling law in [7] is in conflict with our results, which also relay on the Fokker-Planck equation. The origin of the discrepancy is elucidated next.

4. In the work by Takeuchi et al. the scaling law (1) is exclusively derived from the Fokker-Planck equation. This entails moving back and forth between finite and infinite N cases. In particular, Takeuchi et al. assumed that for finite N the Fokker-Planck Eq. (20) remains essentially true replacing λ_∞ by $\lambda(N)$. This assumption is crucial, but questionable, since the growth rate of the Lyapunov vector suffers fluctuations (i.e., diffusion), and there is not a co-moving reference frame (for finite N). In Ref. [7], changing λ_∞ by $\lambda(N)$ modifies $\tilde{P}_s(u)$ as the decay rate α becomes N-dependent. The reasoning proceeds noticing that if N is finite the maximal vector component is about u_{max} such that $\int_{u_{max}}^{\infty} \tilde{P}_s(u)du \sim N^{-1}$. For this scaling relation to hold true it is required that

$$\lambda(N) - \langle \ln \mu \rangle - \ln(1-\epsilon) \simeq \frac{D}{2}(1 + c/\ln N). \qquad (39)$$

Unfortunately, this prediction is already erroneous at leading order. It implies λ_∞ and D are linked through $\lambda_\infty - \langle \ln \mu \rangle - \ln(1-\epsilon) = \frac{D}{2}$, and this yields $\alpha = 1$ for $N \to \infty$, irrespective of the parameter values. These implications are at odds with the numerical evidence, see e.g. Fig. 3.

5. In our work, we have used the Fokker-Planck equation only to get the tail index α of $P_s(v)$ in the thermodynamic limit. The value of λ_∞, and an analytic formula relating $\lambda(N)$ with α and the multipliers' statistics are both derived here independently of the Fokker-Planck equation. This was possible thanks to the positiveness of the multipliers.

6. Our theory predicts the value of λ_∞, which reduces the number of fitting parameters and makes us to be confident with the numerical tests of the theory.

7. It might be argued that, apparently, the numerical results in [7] support the logarithmic scaling law (1). There, however, λ_∞ was a fitting parameter, what, in our experience, introduces a substantial uncertainty and makes it impossible to really distinguish a logarithmic law from a power-law with small exponent γ. When

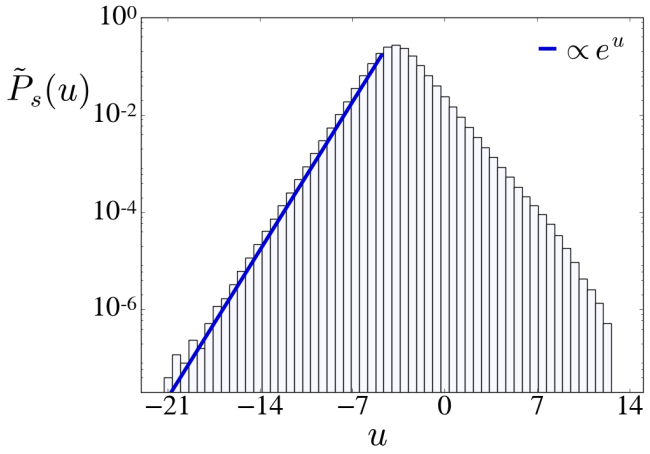

FIG. 11. Probability density $\tilde{P}_s(u)$ obtained form numerical simulations of the RM model with positive and negative multipliers distributed according to a bi-delta density: $\rho_{BD\pm}(\mu) = \frac{1}{b}\delta(\mu - b) + \frac{b-1}{b}\delta[\mu + b/(b-1)]$. This density corresponds to an isolated skewed-tent map. The parameters are the same as in Fig. 3: $\epsilon = 0.02$, $b = 3$. For small $u = \log|v|$, $\tilde{P}_s(u) \propto e^u$, or equivalently $P_s(|v| \to 0) = \text{const}$.

λ_∞ is theoretically known, as we have shown here, the power-law scaling can be established— with an exponent that is model parameter dependent— in regimes I and II, or even a more involved functional form in regime III.

All in all, we conclude that the actual scaling law (or laws) for turbulent GCMs with multipliers adopting both signs remains an open problem. For comparison, we note that in standard one-dimensional coupled-map lattices the sign of the multipliers does not play a significant role. In fact, for an asymptotically small coupling ϵ, the LE always varies as $c/\ln\epsilon$ [5]. If the sign of the multipliers changes or not only alters the scaling factor c. In addition, the convergence of the LE with the system size N generically scales as N^{-1}. Remarkably, the theory is based on a mapping of the tangent dynamics to a simple stochastic partial-differential equation, in which all the Lyapunov vector components have the same sign [4, 28].

Should we expect similar insensitivity of the LE with the multipliers sign in GCMs? This is an open problem that deserves a careful scrutiny. At this point our results constitute new evidence of the complex behavior of deceptively simple GCMs.

ACKNOWLEDGMENTS

D.V. acknowledges support by Agencia Estatal de Investigación and Fondo Social Europeo (Spain) under the doctoral fellowship No. BES-2017-081808 of the FPI Programme. We acknowledge support by Agencia Estatal de Investigación and Fondo Europeo de Desarrollo Regional under Project No. FIS2016-74957-P (AEI/FEDER, EU).

APPENDIX: DERIVATION OF EQ. (30) AND NUMERICAL TESTS

For simplicity, we start approximating $\bar{\mu}$ by $\langle\mu\rangle$ in Eq. (28), and re-write it in terms of the deviations from the expected muliplier value $\delta\mu_j^t = \mu_j^t - \langle\mu\rangle$:

$$\lambda(N) \simeq \lambda_\infty + \left\langle \ln\left[1 + \frac{1-\epsilon}{\langle\mu\rangle}\frac{\sum_{j=1}^N \delta\mu_j^t v_j^t}{\sum_{j=1}^N v_j^t}\right]\right\rangle \qquad \text{(A1)}$$

If N is large we can Taylor expand the logarithm: $\ln(1+x) = x - x^2/2 + \cdots$, where the first order of the expansion is zero, and we truncate at second order:

$$\lambda_\infty - \lambda(N) \simeq \frac{(1-\epsilon)^2}{2\langle\mu\rangle^2}\left\langle\left(\frac{\sum_{j=1}^N \delta\mu_j^t v_j^t}{\sum_{j=1}^N v_j^t}\right)^2\right\rangle \qquad \text{(A2)}$$

The numerator of the average in the right-hand side can be further simplified. Given that the $\delta\mu_j^t$ are completely uncorrelated and have zero mean, we can expand the square and cancel out all (covariance-like) cross-products. Doing so we get this expression:

$$\lambda_\infty - \lambda(N) \simeq \frac{(1-\epsilon)^2}{2\langle\mu\rangle^2}\left\langle\frac{\sum_{j=1}^N (\delta\mu_j^t)^2 (v_j^t)^2}{\left(\sum_{j=1}^N v_j^t\right)^2}\right\rangle \qquad \text{(A3)}$$

The average in the right-hand side, denoted Ψ for short, is far from trivial. As a first check, we represent in Fig. 12(a) the two sides of this equation with data obtained from numerical simulations of the RM model with the bi-delta density. Several values of parameter b were selected as well as a common coupling constant $\epsilon = 0.02$. For the larger b values we may appreciate deviations from the bisectrix, which can only be attributed to the slow convergence of the Taylor expansion of the logarithm. Indeed, our numerical tests of Eq. (A1) yield a quasi perfect agreement between theory and data for all b values. This evidences the risk of relying on numerical simulations alone, given that the asymptotic regime shows up at prohibitively large system sizes for some parameter values. In the particular case of the bi-delta density, it is already difficult to observe the asymptotic decay for b above 4.

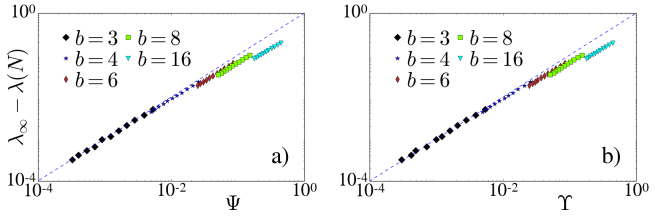

FIG. 12. Numerical tests of Eq. (A3) (a) and Eq. (30) (b) for the bi-delta RM model with $\epsilon = 0.02$ and $b = \{3, 4, 6, 8, 16\}$. (a) The label Ψ in the x-axis stands for the right-hand side of Eq. (A3). The data progressively deviate from the bisectrix (dashed line) as b increases. For each value of b the left most point corresponds to the largest size $N = 102400$ (b) The same as (a), but now Υ in the x-axis denotes the right-hand side of Eq. (30).

If the multipliers do not exhibit large fluctuations we can approximate $(\delta\mu_j^t)^2$ by the variance of μ, and obtain Eq. (30) In Fig. 12(b) we test Eq. (30) setting $\epsilon = 0.02$ and the bi-delta density (8) for several values of b. The results are comparable to those in Fig. 12(a), evidencing that putting the variance of μ out of the average does not deteriorate the accuracy of the approximation.

[1] P. Bergé, Y. Pomeau, and C. Vidal, *Order within Chaos* (Wiley, New York, 1986).

[2] M. Cencini, F. Cecconi, and A. Vulpiani, *Chaos: From Simple*

Models to Complex Systems, Advances in Statistical Mechanics (Book 17) (World Scientific, Singapore, 2010).

[3] T. Bohr, M. H. Jensen, G. Paladin, and A. Vulpiani, *Dynamical Systems Approach to Turbulence* (Cambridge, Cambridge, 1988).

[4] A. Pikovsky and A. Politi, Dynamic localization of Lyapunov vectors in spacetime chaos, Nonlinearity **11**, 1049 (1998).

[5] F. Cecconi and A. Politi, An analytic estimate of the maximum Lyapunov exponent in products of tridiagonal random matrices, J. Phys. A: Math. Gen. **32**, 7603 (1999).

[6] T. Shibata, T. Chawanya, and K. Kaneko, Noiseless collective motion out of noisy chaos, Phys. Rev. Lett. **82**, 4424 (1999).

[7] K. A. Takeuchi, H. Chaté, F. Ginelli, A. Politi, and A. Torcini, Extensive and subextensive chaos in globally coupled dynamical systems, Phys. Rev. Lett. **107**, 124101 (2011).

[8] K. Kaneko, Clustering, coding, switching, hierarchical ordering, and control in a network of chaotic elements, Physica D **41**, 137 (1990).

[9] K. Kaneko, From globally coupled maps to complex-systems biology, Chaos **25**, 097608 (2015).

[10] K. Kaneko, Globally coupled chaos violates the law of large numbers but not the central-limit theorem, Phys. Rev. Lett. **65**, 1391 (1990).

[11] A. S. Pikovsky and J. Kurths, Do globally coupled maps really violate the law of large numbers?, Phys. Rev. Lett. **72**, 1644 (1994).

[12] N. Nakagawa and T. S. Komatsu, Collective motion occurs inevitably in a class of populations of globally coupled chaotic elements, Phys. Rev. E **57**, 1570 (1998).

[13] J. Losson, S. Vannitsem, and G. Nicolis, Aperiodic mean-field evolutions in coupled map lattices, Phys. Rev. E **57**, 4921 (1998).

[14] T. Shibata and K. Kaneko, Collective chaos, Phys. Rev. Lett. **81**, 4116 (1998).

[15] M. Cencini, M. Falcioni, D. Vergni, and A. Vulpiani, Macroscopic chaos in globally coupled maps, Physica D: Nonlinear Phenomena **130**, 58 (1999).

[16] K. A. Takeuchi and H. Chaté, Collective Lyapunov modes, J. Phys. A: Math. Theor. **46**, 254007 (2013).

[17] A. Pikovsky and A. Politi, *Lyapunov exponents* (Cambridge University Press, 2016).

[18] V. I. Oseledets, A multiplicative ergodic theorem. Lyapunov characteristic numbers for dynamical systems, Trans. Moscow Math. Soc. **19**, 197 (1968).

[19] H. Cohn and P. Hall, On the limit behaviour of weighted sums of random variables, Z. Wahrscheinlichkeitstheorie verw. Gebiete **59**, 319 (1982).

[20] H. Daido, Coupling Sensitivity of Chaos, Prog. Theor. Phys. **72**, 853 (1984).

[21] This is tantamount assuming that the diffusion coefficient accompanying chaotic amplification vanishes in the large size limit. This is a plausible assumption, since so far this has been found to be violated only for some Hamiltonian lattices [29].

[22] In [7], the transformation $u_i^t = \ln |v_i^t|$ is taken without paying much attention to the absolute value. This is not completely unreasonable if one considers that in spatio-temporal chaos the absolute value causes no effect in the universality class and thereupon the associated critical exponents [4].

[23] D. L. McLeish and G. L. O'Brien, The expected ratio of the sum of squares to the square of the sum, Ann. Probab. **10**, 1019 (1982).

[24] H. Albrecher and J. Teugels, Asymptotic analysis of a measure of variation, Theory Probab. Math. Stat. **74**, 1 (2007).

[25] H. Fujisaka, Theory of diffusion and intermittency in chaotic systems, Prog. Theor. Phys. **71**, 513 (1984).

[26] P. V. Kuptsov and A. Politi, Large-deviation approach to space-time chaos, Phys. Rev. Lett. **107**, 114101 (2011).

[27] D. Pazó, J. M. López, and A. Politi, Universal scaling of Lyapunov-exponent fluctuations in space-time chaos, Phys. Rev. E **87**, 062909 (2013).

[28] D. Pazó, I. G. Szendro, J. M. López, and M. A. Rodríguez, Structure of characteristic Lyapunov vectors in spatiotemporal chaos, Phys. Rev. E **78**, 016209 (2008).

[29] D. Pazó, J. M. López, and A. Politi, Diverging fluctuations of the Lyapunov exponents, Phys. Rev. Lett. **117**, 034101 (2016).